

## Vapor-Phase Transport as A Novel Route to Hyperbranched Polyamine-Oxide Hybrid Materials

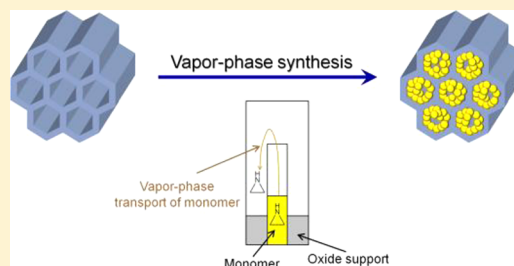
Watcharop Chaikittisilp,<sup>†</sup> Stephanie A. Didas, Hyung-Ju Kim, and Christopher W. Jones\*

School of Chemical &amp; Biomolecular Engineering, Georgia Institute of Technology, 311 Ferst Drive, Atlanta, Georgia 30332-0100, United States

## S Supporting Information

**ABSTRACT:** A new method to prepare hyperbranched polyamine-oxide hybrid materials by means of a vapor-phase transport is developed. In this method, hybrid materials having hyperbranched amine polymers covalently bound to an oxide support are formed by exposing the oxide support to the vapor of small nitrogen-containing heterocyclic monomers, in contrast to the conventional liquid-phase method, in which the support is dispersed in an organic solution containing monomer species. The aziridine and azetidine monomers are polymerized on the surface of the oxide supports (i.e., silica and alumina), resulting in poly(ethylenimine) or poly(propylenimine) chains attached to the porous solid support. The results suggest that the hybrid materials can be prepared over a wide range of preparation conditions with organic contents comparable to or even higher than those obtained from the standard liquid-phase method. It is demonstrated that supports with more acidity result in the hybrid materials with higher organic content. Interestingly, the resulting supported polyamines have lower molecular weights than the previously reported materials prepared by the liquid-phase method. It is anticipated that the vapor-phase synthesis can be applied for the efficient introduction of polyamines into structural forms of supports such as fibers, membranes, and monoliths, for which the liquid-phase method may be inappropriate or inefficient.

**KEYWORDS:** hyperbranched aminosilica, supported polyamine, poly(ethylenimine), poly(propylenimine), organic–inorganic hybrid, ring-opening polymerization, class 3 CO<sub>2</sub> adsorbent, PEI, PPI



## ■ INTRODUCTION

Porous organic–inorganic hybrid materials are of growing interest because their applications can be expanded beyond the traditional scope of organic or inorganic components alone. The organic functionalization of porous oxide frameworks, mostly demonstrated to date on silica-based materials, can offer not only new functions but also additional synergistic properties created by specific interactions at the hybrid interfaces.<sup>1</sup> In particular, functionalization of mesoporous silica with amino groups has been intensively studied because these materials can be applied in a wide variety of applications including catalysis, adsorption of heavy metal cations, immobilization of drugs and biomolecules, and CO<sub>2</sub> capture.<sup>2–5</sup>

Incorporation of amine moieties into/onto the support frameworks has been achieved mostly via four liquid-phase synthetic routes: (i) physical impregnation of monomeric or polymeric amines into/onto the porous supports, (ii) covalent grafting of amines, most often organosilanes with pendant amino groups, onto the support surfaces, (iii) direct co-condensation of amine-containing molecules and conventional precursors during materials syntheses, and (iv) in situ polymerization of amine-containing monomers in the pores of supports, with the latter three methods resulting in amines or aminopolymers covalently bound to the supports.<sup>1</sup>

Among the aforementioned methods, in situ polymerization to produce polyamines can provide strong covalent links

between the amines and the supports while providing high loadings of amine groups, although very large polymer loadings can sometimes remove or block the porosity. Ring-opening polymerization of cyclic monomers onto the support surfaces can be applied for various polymers including polypeptides<sup>6</sup> and poly(ethylenimine).<sup>7,8</sup> Small nitrogen-containing heterocycles having high ring strain such as aziridine (three-membered ring) and azetidine (four-membered ring) can undergo nucleophilic ring-opening polymerization to generate polyamines on the surface or in the pores of porous oxides with very high yields (see Scheme 1).<sup>9</sup>

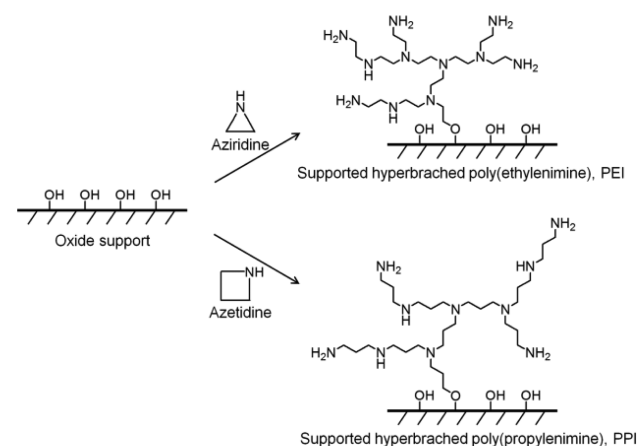
Among others, our group has developed a simple way to prepare supported poly(ethylenimine) materials by ring-opening polymerization of aziridine in the presence of porous silicates as supports in organic solvent media (Scheme 1).<sup>7,8,10</sup> These materials, which have been referred to as hyperbranched aminosilica (HAS) materials, have been used as adsorbents for the selective removal of oxygenates from bio-oil<sup>11</sup> and for CO<sub>2</sub> capture from flue gas and ambient air.<sup>8,12</sup> Although the HAS materials showed excellent performance in CO<sub>2</sub> capture from humid gas streams under a lab-scale, packed bed configuration, heat and mass transfer resistances associated with the

Received: December 7, 2012

Revised: January 22, 2013

Published: January 25, 2013

**Scheme 1. Ring-Opening Polymerization of Aziridine and Azetidine onto the Oxide Support**



exothermic chemisorption of CO<sub>2</sub> on polyamines and hindered diffusion in polymer-filled pores may prohibit packed bed operation at a commercial scale.<sup>5a,13</sup> For HAS and related adsorbents to be utilized for large-scale CO<sub>2</sub> capture, the use of structured contactors such as hollow fibers, nanofibers, and honeycomb monoliths as support materials has been proposed to resolve some of these problematic issues associated with flowing large volumes of CO<sub>2</sub>-containing gas over these materials.<sup>13a,14</sup> However, preparation of aminosilica hybrid materials, including HAS materials, typically requires reaction in a condensed phase using liquid reagents or solvents. Functionalization of the structured contactors, such as monoliths, via such liquid-phase polymerization techniques is difficult to carry out on a large scale.

As is widely known, small nitrogen-containing heterocycles can be vaporized even at ambient conditions because of their low boiling points.<sup>9</sup> We have thus considered that vapors of such heterocyclic molecules should effectively transport or diffuse into the interiors of the structured contactors, and that vapor-phase polymerization techniques may therefore be possible. If the internal surface of contactors contains suitable polymerization initiators, ring-opening polymerization should spontaneously occur under appropriate conditions, resulting in contactor-supported polymers. Related approaches have been applied to prepare thin films of conducting polymers,<sup>15</sup> mesoporous silicas,<sup>16</sup> and mesoporous metals,<sup>17</sup> in which monomers or reductants were transported and infiltrated through the vapor phase onto the substrates.

We describe herein a novel synthetic route to prepare hyperbranched polyamine-oxide hybrid materials through vapor-phase transport. In this method, the small nitrogen-containing heterocyclic monomers are transported into/onto the solid supports in the vapor phase and subsequently polymerization is initiated at the support surface. The amount of polyamines formed on the supports can be affected by several synthesis parameters including temperature, reaction time, and the acidity of supports. In comparison to the conventional liquid-phase method, this novel vapor-phase method is anticipated to be more efficient in introduction of polyamines into the structured contactors, and may prove to be a more scalable technique to create important CO<sub>2</sub> adsorbents. To the best of our knowledge, polyamine-oxide hybrid materials are successfully prepared here via the vapor-phase method for the first time.

## EXPERIMENTAL SECTION

**Chemicals.** The following reagents were obtained from the commercial suppliers and used as received without further purification: 2-chloroethylamine hydrochloride (Aldrich, 99%), sodium hydroxide (EMD, ACS grade, 97%), azetidide hydrochloride (Aldrich, 97%), potassium hydroxide (Fluka, purum ≥85%), Pluronic P123 EO<sub>20</sub>-PO<sub>70</sub>-EO<sub>20</sub> triblock copolymer (Aldrich), concentrated hydrochloric acid (Sigma-Aldrich), tetraethyl orthosilicate (Aldrich, 98%), aluminum isopropoxide (Aldrich), 2 N hydrochloric acid (BDH), methanol (BDH), acetone (BDH), activated acidic aluminum oxide (Sigma-Aldrich, Brockmann I), activated basic aluminum oxide (Sigma-Aldrich, Brockmann I), activated neutral aluminum oxide (Sigma-Aldrich, Brockmann I), water (Fluka, TraceSELECT), sodium sulfate (Sigma-Aldrich, 99+%), acetic acid (Sigma-Aldrich, glacial), and poly(ethylenimine)s (Aldrich,  $M_w = 800, 1300, 2000, 25000$ ;  $M_n = 600, 1200, 1800, 10000$ ; Polysciences,  $M_w = 1800$ ).

**Synthesis of Aziridine.** Aziridine was synthesized from 2-chloroethylamine according to the previous report<sup>8a</sup> with some modifications in the purification step. To a 250-mL round-bottom flask containing 2-chloroethylamine hydrochloride (30 g) was added a sodium hydroxide aqueous solution (25.8 g of sodium hydroxide in 170 g of deionized water). The resultant solution was heated to 50 °C and stirred at this temperature for 2 h. Aziridine was then recovered by a partial static vacuum distillation at 75 °C. The collected distillate was dried over sodium hydroxide pellets and kept in a freezer overnight. Aziridine phase-separated as an upper layer of liquid and was recovered. The purified aziridine was obtained as a colorless oil in 70–80% yield and stored in a freezer. <sup>1</sup>H NMR (400.0 MHz, (CD<sub>3</sub>)<sub>2</sub>SO, TMS):  $\delta$  (ppm) 1.17, 1.53; <sup>13</sup>C NMR (100.6 MHz, (CD<sub>3</sub>)<sub>2</sub>SO, TMS):  $\delta$  (ppm) 17.4.

**Preparation of Azetidide.** Azetidide was prepared by distillation of azetidide hydrochloride over potassium hydroxide.<sup>18</sup> To a 100-mL round-bottom flask was added potassium hydroxide (7.1 g) and deionized water (4 mL). The mixture was stirred until potassium hydroxide was completely dissolved. Then, 5 g of azetidide hydrochloride was added to the stirred potassium hydroxide solution. Azetidide was isolated by distillation and stored in a freezer. <sup>1</sup>H NMR (400.0 MHz, CDCl<sub>3</sub>, TMS):  $\delta$  (ppm) 1.99, 2.25, 3.55; <sup>13</sup>C NMR (100.6 MHz, CDCl<sub>3</sub>, TMS):  $\delta$  (ppm) 22.1, 48.2.

**Caution!** Aziridine and azetidide are highly reactive and toxic. Use extreme caution when handling these compounds. Only handle in a well-ventilated fume hood and always wear proper personal protective equipment.

**Synthesis of SBA-15 Mesoporous Silica.** SBA-15 silica supports were synthesized by using a modified, previously reported method,<sup>19</sup> scaling the ingredients accordingly. In a typical procedure, pluronic P123 triblock copolymer (12 g), concentrated hydrochloric acid (72 g), and deionized water (328 g) were mixed in a 1-L Erlenmeyer flask. After being stirred for 5 h at 40 °C, 25.4 g of tetraethyl orthosilicate was added to the stirred solution. The resultant mixture was stirred for 21 h at 40 °C, producing a cloudy solution with a white precipitate. Subsequently, this mixture was heated statically at 100 °C for 24 h. SBA-15 material was isolated by filtration and washed with a copious amount of deionized water. The obtained white solid was dried at 75 °C overnight. The organic template was removed by calcination at 550 °C for 6 h with an intermediate step at 150 °C for 2 h (a heating rate of 1 °C min<sup>-1</sup>).

**Incorporation of Aluminum into SBA-15.** The acidity of SBA-15 material was modified by postsynthetic grafting of aluminum species onto the SBA-15 surface.<sup>20</sup> Briefly, the aluminate solution was prepared by dissolving 0.26 g of aluminum isopropoxide in 60 mL of 0.03 M hydrochloric acid. After being stirred at room temperature for 6 h, to the aluminate solution was added 1.5 g of the calcined SBA-15. The suspension was stirred at room temperature for 18 h. The suspension was filtered and washed with deionized water. The recovered solid was dried at 75 °C overnight and then calcined at 550 °C for 6 h with an intermediate step at 150 °C for 2 h (a heating rate of 1 °C min<sup>-1</sup>).

Table 1. Physical and Chemical Characteristics of the Hyperbranched Poly(ethylenimine)-Oxide Hybrids Prepared on SBA-15

sample	synthesis condition			organic loading (wt %) <sup>b</sup>	amine content (mmol g <sup>-1</sup> )		$S_{\text{BET}}$ (m <sup>2</sup> g <sup>-1</sup> ) <sup>d</sup>	$V_{\text{Ttotal}}$ (cm <sup>3</sup> g <sup>-1</sup> ) <sup>e</sup>	percent occupancy (%) <sup>f</sup>	remaining $V_{\text{g}} - V_{\text{g}}^{\text{support}}$ (cm <sup>3</sup> g <sup>-1</sup> ) <sup>g</sup>
	temp. (°C)	ratio <sup>a</sup>	time (h)		$N_{\text{TGA}}$ <sup>b</sup>	$N_{\text{EA}}$ <sup>c</sup>				
S-70C-1-24h	70	1	24	26.6	6.19	5.51	214	0.42	32.6	0.04
S-70C-2-24h	70	2	24	31.1	7.23	6.61	182	0.33	40.6	0.05
S-70C-3-24h	70	3	24	38.6	8.98	8.43	40	0.11	56.5	0.19
S-70C-4-24h	70	4	24	41.5	9.66	8.97	22	0.07	63.8	0.17
S-23C-4-24h	23	4	24	15.7	3.66	3.32	372	0.62	16.8	0.01
S-23C-4-168h	23	4	168	27.2	6.33	5.74	233	0.42	33.6	0.03
S-50C-4-24h	50	4	24	31.7	7.38	6.98	174	0.32	41.7	0.04
S-50C-4-48h	50	4	48	39.9	9.27	8.55	30	0.08	59.6	0.20
S-60C-4-24h	60	4	24	35.0	8.15	7.60	67	0.15	48.5	0.22
S-80C-4-24h	80	4	24	42.3	9.83	9.19	21	0.07	65.8	0.14

<sup>a</sup>The mass ratio of aziridine/support. <sup>b</sup>Determined by TGA. <sup>c</sup>Determined by elemental analysis. <sup>d</sup>Surface area calculated by the BET method. <sup>e</sup>Total pore volume at  $P/P_0 = 0.99$ . <sup>f</sup>Calculated by dividing the estimated volume of polyamine (in cm<sup>3</sup> of polymer per gram of support) by the total pore volume of bare support, assuming a polyamine density of 1.05 g cm<sup>-3</sup>. <sup>g</sup>Remaining pore volume = [pore volume of bare support] - [pore volume of hybrid material] - [volume of polyamine].<sup>5c,8b</sup>

### Preparation of Hyperbranched Polyamine-Oxide Hybrids via Vapor-Phase Transport.

For the laboratory scale experiment, polymerization of aziridine on the oxide supports via vapor-phase transport was carried out in a 15-mL glass pressure tube. Typically, the support materials were hand-ground by a mortar and pestle and then dried at 105 °C for at least 48 h. About 0.15 g of the well ground and dried supports was added into the pressure tube. A small glass test tube (12 × 75 mm, VWR) containing a different amount of aziridine was then placed inside the pressure tube (see Supporting Information, Figure S1). The pressure tube was closed tightly and heated to a desired temperature for a specified period of reaction time. The reaction was quenched by adding the pressure tube into an ice bath. The solid sample was washed with excess amounts of methanol (100 mL × 3) and acetone (100 mL × 3) to remove the physisorbed aziridine and polyamines from the sample surface and then recovered by filtration. The resulting solid was dried under high vacuum at room temperature overnight. The resulting hyperbranched poly(ethylenimine)-oxide hybrids were denoted as *W-XC-Y-Zh*, where *W* represents the oxide supports, *X* represents the synthesis temperature, *Y* represents the aziridine-to-support mass ratio, and *Z* represents the synthesis time. The oxide supports included SBA-15, Al-grafted SBA-15, acidic alumina, basic alumina, and neutral alumina, which are referenced as S, AS, AA, BA, and NA, respectively. For example, S-50C-4-24h refers to the hybrid material prepared on the SBA-15 support with the aziridine/SBA-15 mass ratio of 4 at 50 °C for 24 h. The hyperbranched poly(propylenimine)-oxide hybrids were also prepared using the same procedures from azetidione monomers.

**Removal of Polyamines from Silica Supports.** The supported polyamines were cleaved from the solid support by alkali treatment. This removal procedure would be universal for any supports that can be dissolved in alkaline media. About 0.5 g of supported polyamines was dispersed in 100 mL of deionized water. Then, 35 g of potassium hydroxide was added to the dispersion. The resulting mixture was stirred at 50 °C for 24 h, after which the support was degraded into soluble species. At least 70 g of water was removed by rotary evaporation at about 60 °C. The remaining solution was kept in a freezer overnight. The polyamines appearing as viscous liquid were phase-separated as an upper layer of the mixture and mechanically recovered by a spatula for further analyses.

**Characterization.** Powder X-ray diffraction (XRD) patterns were collected on a Philips X'pert diffractometer using Cu K $\alpha$  radiation. Nitrogen adsorption-desorption was performed on a Micromeritics TriStar II 3020 at -196 °C. Before the measurement, the samples were degassed at 110 °C under vacuum for at least 8 h. Pore size distribution was calculated by a nonlocal density functional theory (NL-DFT) by using the silica cylindrical pore, equilibrium model.<sup>21</sup> Scanning electron microscope (SEM) images were taken from an LEO

1530 instrument. Organic loadings were determined by thermogravimetric analysis (TGA) using a Netzsch STA409 instrument. Samples were heated under a mixed gas stream of air (90 mL min<sup>-1</sup>) and nitrogen (30 mL min<sup>-1</sup>) with a heating rate of 10 °C min<sup>-1</sup>. The amine loading was estimated from relative weight loss in the range of 150–600 °C. The organic contents were first estimated by TGA,<sup>22</sup> and these values were then verified by elemental analyses (EA). Inductively Coupled Plasma-Optical Emission Spectroscopy (ICP-OES) was used to determine the aluminum content in the supports. EA and ICP-OES experiments were performed by Columbia Analytical Services (Tucson, AZ). Samples were dried under vacuum prior to analysis at 80 °C.<sup>27</sup> Al solid-state magic-angle spinning (MAS) nuclear magnetic resonance (NMR) experiments were carried out on a Bruker DSX 300 spectrometer at a frequency of 78.2 MHz. The sample was spun at 5 kHz with a single pulse of  $\pi/6$  and a recycle delay of 0.5 s. Solution-state NMR spectra were recorded on a Varian Mercury Vx400 spectrometer. Inversely gated solution-state <sup>13</sup>C NMR was used to determine the ratios of primary, secondary, and tertiary amines. A proton decoupled technique with a relaxation time of 4 s allows for quantitative analysis of the cleaved polymers.<sup>23</sup> Samples were prepared in D<sub>2</sub>O with a drop of chromium(III) acetylacetonate in deuterated dimethylsulfoxide (DMSO) to aid relaxation and minimize interference from residual silica or base after cleavage. Spectra were recorded using 12,000 scans on a Bruker DRX 500 spectrometer. Molecular weights of cleaved polyamines were estimated by aqueous gel permeation chromatography with a system composed of a Shimadzu LC-20AD pump, a Shimadzu RID-10A RI detector, a Shimadzu SPD-20A UV detector, a Shimadzu CTO-20A column oven, and Tosoh Bioscience TSKgel PWXL Guard, Viscotek Viscogel G6000 and G4000 columns mounted in series. The mobile phase consisted of 0.5 M acetic acid and 0.3 M Na<sub>2</sub>SO<sub>4</sub>, and the flow rate was maintained at 0.4 mL min<sup>-1</sup>.

**CO<sub>2</sub> Adsorption Measurement.** A TA Q500 thermogravimetric analyzer was used to assess CO<sub>2</sub> adsorption capacities under anhydrous conditions with 10% CO<sub>2</sub> balanced with helium. The hybrid materials were loaded in a platinum pan and pretreated under a helium atmosphere at 110 °C for 3 h with a heating rate of 5 °C min<sup>-1</sup> to remove any preadsorbed CO<sub>2</sub> and water, following by cooling to 25 °C with a rate of 5 °C min<sup>-1</sup> where they were held at this temperature for 1 h to stabilize the sample weight and temperature before introducing the CO<sub>2</sub>-containing gas. Adsorption experiments were started by exposing the samples to a dry CO<sub>2</sub> gas mixture for 6 h. The adsorption capacities were calculated from the weight gain after the CO<sub>2</sub> exposure.

## RESULTS AND DISCUSSION

**Effects of Synthesis Parameters.** The solid support and liquid aziridine were put separately inside the reaction vessel, which was heated at a prescribed temperature for a fixed time. After synthesis, no accumulated liquid aziridine was found in the solid support container, suggesting that the solid support was contacted directly with aziridine in the vapor phase only, not liquid aziridine. The recovered solids were washed extensively with organic solvents to remove physisorbed monomer or polymer species (600 mL per 0.15 g of initial solid support). To study the feasibility of this novel method, poly(ethylenimine)s were prepared on SBA-15 mesoporous silica as the solid support (see Supporting Information, Figure S2 for the detailed characterization of SBA-15)<sup>24</sup> under varied synthesis parameters, as summarized in Table 1. We first studied the effects of the aziridine-to-support mass ratio by fixing the synthesis temperature and time at 70 °C and 24 h, respectively. This temperature is higher than the boiling point of aziridine (56.7 °C);<sup>9b</sup> therefore, aziridine should be vaporized inside the vessel efficiently. The mass of poly(ethylenimine) formed increased as the mass ratio was increased, with the highest organic loading reaching 41.5 wt % at an aziridine/support mass ratio of 4 (see Table 1). Powder XRD patterns of the obtained hybrids are shown in Figure 1a.

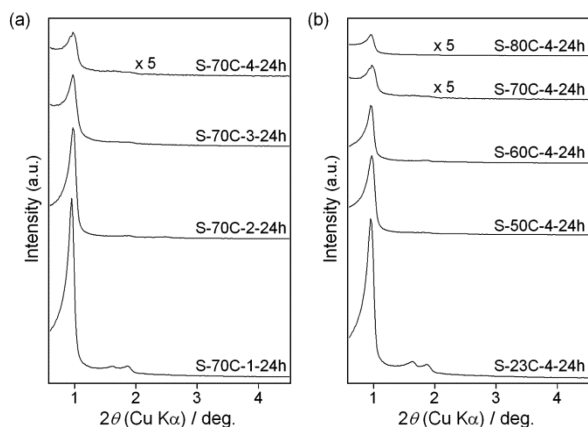


**Figure 1.** Powder XRD patterns of the resulting hyperbranched poly(ethylenimine)-oxide hybrids synthesized at different aziridine-to-support ratios (a) and at different synthesis temperatures (b).

The S-70C-1-24h sample clearly exhibits XRD peaks with (100), (110), and (200) reflections, which are characteristic of the two-dimensional (2D) hexagonal mesostructure of the SBA-15 support. The intensity of the XRD peaks decreased as the ratios increased, consistent with the increasing amount of polyamines on the support surface. This decrease in peak intensity is a result of a reduction in electron density contrast between the mesopore spaces and the silica pore walls after polymerization, caused by the growth of polyamines in the pore interior. These results also suggest that the ordered mesostructure of the SBA-15 supports was preserved after functionalization.

The porous characteristics of the resulting hybrids were studied by nitrogen adsorption measurements. Figure 2a depicts nitrogen adsorption–desorption isotherms of the hybrid materials, clearly showing IUPAC type IV isotherms with hysteresis indicative of mesoporous materials, especially for the samples with lower organic loadings. The apparent Brunauer–Emmett–Teller (BET) specific surface areas

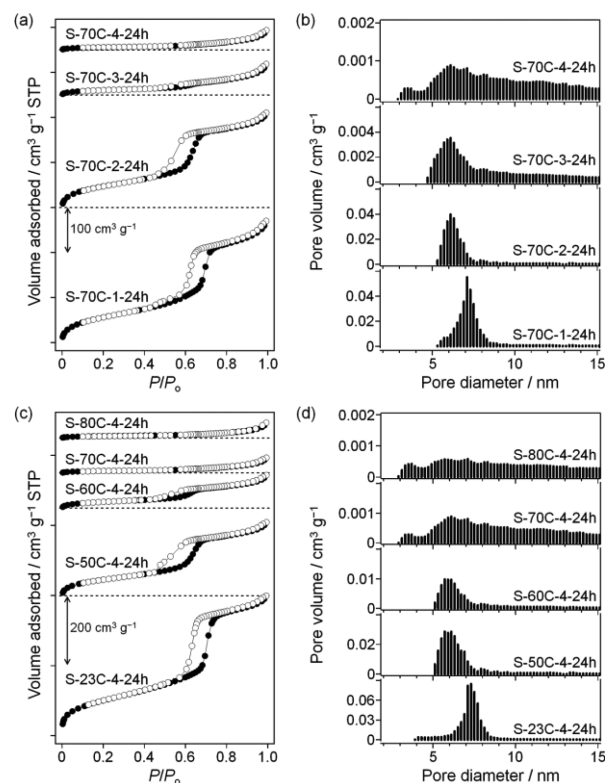


**Figure 2.** (a,c) Nitrogen sorption isotherms (filled and empty symbols representing adsorption and desorption branches, respectively) and (b,d) the corresponding histograms of NL-DFT pore size distribution of the resulting hybrids. In (a), the isotherms of S-70C-2-24h, S-70C-3-24h, and S-70C-4-24h were offset by 300, 550, and 650  $\text{cm}^3 \text{g}^{-1}$  STP, respectively; while in (c), the isotherms of S-50C-4-24h, S-60C-4-24h, S-70C-4-24h, and S-80C-4-24h were offset by 400, 650, 750, and 850  $\text{cm}^3 \text{g}^{-1}$  STP, respectively.

decreased from 214  $\text{m}^2 \text{g}^{-1}$  for the S-70C-1-24h sample to 22  $\text{m}^2 \text{g}^{-1}$  for the S-70C-4-24h sample, while, the total pore volumes (at  $P/P_0 = 0.99$ ) decreased from 0.42 to 0.07  $\text{cm}^3 \text{g}^{-1}$  for the S-70C-1-24h and S-70C-4-24h samples, respectively. Nonlocal density functional theory (NL-DFT) was employed to estimate the pore size distributions of the materials (Figure 2b). It can be seen that the pore diameters of the obtained hybrid materials shifted to smaller sizes, and the pore size distributions became broader when the organic loadings increased. Comparing with the parent SBA-15 support, the reductions of the BET surface area, total pore volume, and pore diameter indicate that at least some portions, if not all of the polyamines, were occluded inside the pore space of the SBA-15 support. SEM images of the parent SBA-15, and the resulting hybrid materials (Supporting Information, Figure S3) reveal that the morphologies and external surfaces of all the samples were similar, thereby further supporting the notion that the majority of polyamines were in the particle interior and not on the external surface of the hybrid materials.

In the next set of experiments, the hybrid materials were prepared with an aziridine/support ratio of 4 at different temperatures for 24 h. As listed in Table 1, the synthesis temperature influenced the organic content of the obtained materials; a higher temperature resulted in the higher organic loadings. The highest loading obtained at the synthesis temperature of 80 °C is slightly higher than the highest loading of the materials synthesized by the conventional liquid-phase

**Table 2. Physical and Chemical Characteristics of the Hyperbranched Poly(ethylenimine)-Oxide Hybrids Prepared on the Al-Grafted SBA-15 and Alumina Supports<sup>a</sup>**

sample	synthesis temp. (°C)	organic loading (wt %) <sup>b</sup>	amine content (mmol g <sup>-1</sup> )		$S_{\text{BET}}^{\text{c}}$ (m <sup>2</sup> g <sup>-1</sup> ) <sup>d</sup>	$V_{\text{Total}}^{\text{e}}$ (cm <sup>3</sup> g <sup>-1</sup> ) <sup>e</sup>	percent occupancy (%) <sup>f</sup>	remaining $V_{\text{support}}^{-\text{h}}$ (cm <sup>3</sup> g <sup>-1</sup> ) <sup>g</sup>
			$N_{\text{TGA}}^{\text{b}}$	$N_{\text{EA}}^{\text{c}}$				
<i>Samples Prepared on the Al-Grafted SBA-15 Supports</i>								
AS-23C-4-24h	23	16.0	3.73	3.36	307	0.54	20.4	0.00
AS-50C-4-24h	50	32.3	7.52	7.24	57	0.13	51.1	0.18
AS-60C-4-24h	60	36.8	8.57	8.69	19	0.06	62.4	0.18
AS-70C-4-24h	70	43.5	10.12	9.53	17	0.05	82.4	0.00
AS-80C-4-24h	80	46.8	10.89	10.36	16	0.05	94.2	-0.12
<i>Samples Prepared on the Alumina Supports</i>								
AA-50C-4-24h	50	15.2	3.54	n.d. <sup>h</sup>	24	0.06	74.4	-0.01
NA-50C-4-24h	50	4.8	1.12	n.d. <sup>h</sup>	128	0.21	20.1	-0.03
BA-50C-4-24h	50	3.9	0.91	n.d. <sup>h</sup>	139	0.21	15.4	-0.02

<sup>a</sup>The aziridine/support mass ratio and synthesis time were set at 4 and 24 h, respectively. <sup>b</sup>Determined by TGA. <sup>c</sup>Determined by elemental analysis. <sup>d</sup>Surface area calculated by the BET method. <sup>e</sup>Total pore volume at  $P/P_0 = 0.99$ . <sup>f</sup>Calculated by dividing the estimated volume of polyamine (in cm<sup>3</sup> of polymer per gram of support) by the total pore volume of bare support, assuming the polyamine density of 1.05 g cm<sup>-3</sup>. <sup>g</sup>Remaining pore volume = [pore volume of bare support] - [pore volume of hybrid material] - [volume of polyamine]. <sup>h</sup>Not determined.

method reported previously,<sup>7,8</sup> suggesting that this vapor-phase method can be as useful as the liquid-phase method for the introduction of hyperbranched polyamines into the mesoporous supports. Interestingly, materials with a significant organic content can also be prepared even at room temperature. The synthesis time also affected the organic loading, with a longer reaction time resulting in higher organic loading (e.g., S23C-4-24h versus S23C-4-168h).

Powder XRD patterns of the obtained hybrids shown in Figure 1b reveal a 2D hexagonal mesostructure, suggesting that the ordered mesostructure of the supports was retained after the functionalization. Nitrogen adsorption-desorption isotherms and the corresponding NL-DFT pore size distributions of the obtained hybrid materials prepared at different temperatures are shown in Figure 2c and d, respectively. The BET surface areas and total pore volumes were calculated to vary from 372 to 21 m<sup>2</sup> g<sup>-1</sup> and from 0.62 to 0.07 cm<sup>3</sup> g<sup>-1</sup>, respectively, depending on the polyamine loadings. Again, the NL-DFT pore diameters shifted to smaller sizes and the pore size distributions became broader when the organic loadings increased. The decreases in BET surface area, total pore volume, and pore diameter suggest that the polyamines are formed in the interiors of the SBA-15 support, as noted above.

In the hybrid materials with low organic loadings (up to about 30 wt %), the hystereses were essentially parallel for the adsorption and desorption branches. In addition, the NL-DFT pore size distributions were relatively narrow. These data suggest that most of polyamines were well-dispersed inside the pores of the supports and likely grown via a layer-by-layer fashion. On the contrary, in the hybrid materials with higher organic loadings, the broad NL-DFT pore size distributions suggest that polyamines were likely ill-dispersed inside the pores and some polymers likely formed near/in pore windows, leading to some pore blocking. This phenomenon is also supported by the fact that the total pore volume approached zero at higher organic loading but the occupancy of polyamines reached only about 70% of the total porosity of the bare support (see Table 1).

It is noteworthy that the micropore volumes of all the hybrid materials determined by the  $t$ -plot method became zero or negligible after vapor-phase functionalization, irrespective of the

polyamine loading. This is in contrast with the previously reported materials prepared by liquid-phase reaction,<sup>8b</sup> where some microporosity remained at low amine loadings but disappeared at amine loadings higher than 5.3 mmol N g<sup>-1</sup>. Under the present conditions, polyamines prepared via the vapor-phase method seem to be reactively grown on the oxide surface, and the micropores of the support can accommodate only a small amount of polyamines before the micropores are closed or blocked by the formed polyamines.

The “remaining pore volume” parameter was calculated for the simple assessment of pore closing or blocking as the normalized volume per gram of support by subtracting the pore volume of hybrid material and the estimated volume of polyamine from the pore volume of bare oxide support (i.e., [remaining pore volume] = [pore volume of bare support] - [pore volume of hybrid material] - [volume of grown polyamine]). It was assumed that the polyamines were not grown in the micropores of support and that the polyamine density is equal to the bulk density of poly(ethylenimine).<sup>5c,8b</sup> In an ideal case where all the polyamines are occluded inside the pores, the remaining pore volume should equal zero. A positive value of this parameter means there are some pore spaces inaccessible to nitrogen adsorption at -196 °C, while a negative value suggests that parts of polyamine are likely located on the particle exteriors. It is also possible to have both inaccessible pore spaces and polyamines located on the particle exteriors that can result in positive or negative values, depending on the relative magnitudes of each effect. As shown in Table 1, it is likely that at low organic loadings most of the polyamines were located inside the mesopores of the hybrid materials without the pore blocking, as the remaining pore volumes were close to zero, while at higher organic loadings, the remaining pore volumes became more positive, suggesting some pore blocking. In both cases, the remaining pore volumes suggest that only a small amount, if any, of polyamines were grown on the particle exteriors, consistent with SEM observations.

The thermal stability of the supported polyamines was examined by TGA in the presence of gaseous oxygen. Thermal decomposition or oxidation of the polyamines initiated at about 200 °C with the peak of the first-derivative TG weight (DTG)

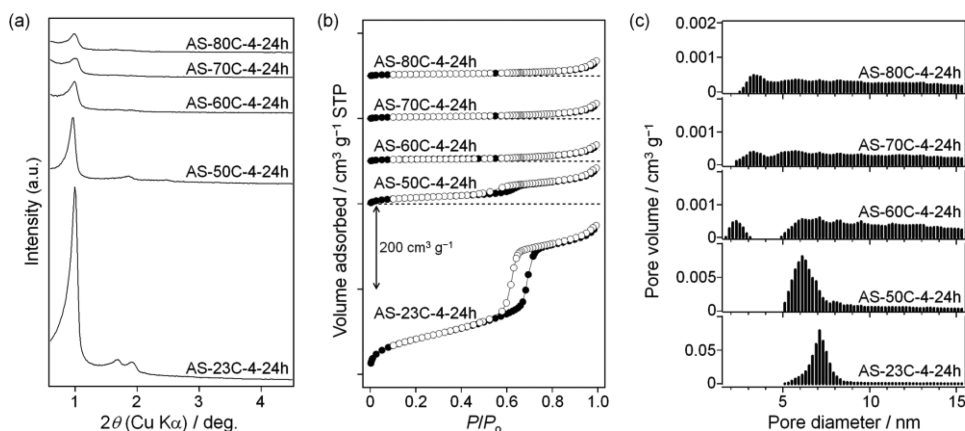


**Figure 3.** (a) Powder XRD patterns, (b) nitrogen adsorption–desorption isotherms (filled and empty symbols representing adsorption and desorption branches, respectively), and (c) the corresponding histograms of NL-DFT pore size distribution of the hyperbranched poly(ethylenimine)-oxide hybrids prepared on the Al-grafted SBA-15 support. The isotherms of AS-50C-4-24h, AS-60C-4-24h, AS-70C-4-24h, and AS-80C-4-24h were offset by 400, 500, 600, and 700  $\text{cm}^3 \text{g}^{-1}$  STP, respectively.

observed at 220 °C (see Supporting Information, Figure S4). These peaks are about 40 °C higher than those of materials prepared by impregnation of poly(ethylenimine) into SBA-15,<sup>3g</sup> suggesting that the resulting supported polyamines are more thermally stable than in the case of physically bound poly(ethylenimine)s. As is generally known, Si–O–C linkages are easily hydrolyzed, particularly under acidic and basic conditions.<sup>25</sup> However, the oxide-supported, hyperbranched polyamine materials have been previously demonstrated to be stable under several conditions containing water vapor,<sup>7,8</sup> although the Si–O–C linkages may be cleaved under harsher environments. The stability against hydrolysis of these materials under hydrous conditions is likely because the Si–O–C linkages are protected from water by bulky hyperbranched polymers (steric effect).<sup>25</sup>

**Effects of Support Acidity.** SBA-15 mesoporous silica supports were functionalized with aluminum by a postgrafting method<sup>20</sup> to investigate the effects of support acidity on supported polyamine synthesis via the vapor-phase transport. The detailed characterization of the Al-grafted SBA-15 support is shown in the Supporting Information, Figure S5.<sup>26</sup> The incorporation of aluminum was confirmed by ICP-OES, with the material having a Si/Al atomic ratio of 29. The nature of the aluminum species was determined by solid-state<sup>27</sup> Al MAS NMR. The spectrum (see Supporting Information, Figure S5b) reveals that Al atoms are located primarily in tetrahedral positions, although nonframework, octahedral Al species also exist.

The hybrid materials prepared on the Al-grafted SBA-15 supports with an aziridine/support ratio of 4 at different temperatures for 24 h are summarized in Table 2. Similar to the hybrids prepared on SBA-15 silica supports, the materials obtained at higher synthesis temperature possessed higher organic loadings, with the highest value obtained being 46.8 wt %, which is to our knowledge the highest loading reported thus far for this class of material.<sup>7,8,10</sup> Under the same synthesis conditions, the hybrid materials prepared on the Al-grafted SBA-15 supports have higher polyamine loadings than those prepared on the pure silica SBA-15, with the different loadings being more pronounced at higher synthesis temperatures, suggesting that the acidity of the supports can enhance the polymerization of the cyclic amines. This was expected, as the polymerization reaction is known to be acid-catalyzed and the

Al-grafted SBA-15 is more acidic than the pure silica parent material.

Powder XRD patterns of the obtained samples are shown in Figure 3a. Similar to the case of SBA-15, the patterns arising from the 2D hexagonal mesostructure were observed, indicating the ordered mesostructure remained in the hybrid materials after the polymerization. Figure 3b and 3c depict the nitrogen adsorption–desorption isotherms and the corresponding NL-DFT pore size distributions of these materials, respectively. At low loadings, parallel hysteresis loops were observed, suggesting the grown polyamines were homogeneously dispersed over the interior of the supports. As the polyamine loadings increased, the NL-DFT pore diameters shifted to smaller pore sizes and the pore size distributions became broader, akin to the silica SBA-15-supported hybrid materials. Quantification of microporosity by the *t*-plot method suggests that the micropores disappear or are inaccessible in the resulting hybrids. The calculated BET surface areas and total pore volumes ranged from 307 to 16  $\text{m}^2 \text{g}^{-1}$  and from 0.54 to 0.05  $\text{cm}^3 \text{g}^{-1}$ , respectively. Interestingly, the maximum occupancy of polyamines reached 94% of the total porosity of the supports, which is much higher than in the case of SBA-15 supports (vide supra).

Plots of total pore volume versus amine content and polyamine occupancy are depicted in Figure 4a and b, respectively. There are clearly two different regions of the plots. At low polyamine loadings, the pore volumes decreased linearly as the content and occupancy of polyamines increased

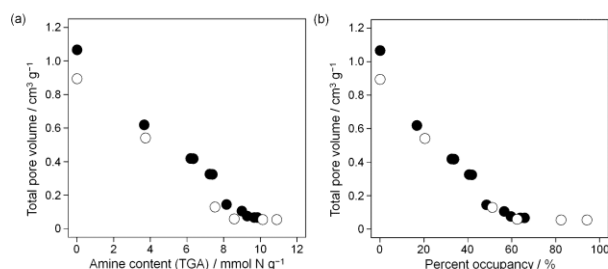


**Figure 4.** Total pore volume of the hyperbranched poly(ethylenimine)-oxide hybrids prepared on the SBA-15 (filled symbols) and the Al-grafted SBA-15 (empty symbols) supports as function of (a) amine contents and (b) percent occupancy.

up to certain values (about 9 mmol N g<sup>-1</sup> for amine content and 60% occupancy) before the pore spaces (or pore openings) became saturated. After passing this point, decreases in pore volume were very small as additional polymers were added. In the former region, most polyamines seem to be grown quasi-homogeneously and none of pores appear blocked or closed. In the latter part where the pore apertures were almost closed, additional polyamines that were formed likely attached near the pore apertures or outer surface and accordingly some pore blocking occurred.

The effects of support acidity were further studied on mesoporous activated alumina supports. The textural properties of the acidic, neutral, and basic alumina supports used here are nearly identical;<sup>27</sup> therefore, the effect of surface acid/base characteristics can be clearly elucidated. The poly(ethylenimine)–alumina hybrid materials were synthesized with an aziridine/support mass ratio of 4 at 50 °C for 24 h. As summarized in Table 2, the polyamines were formed on the acidic alumina support with about 75% occupancy whereas the neutral and basic alumina could accommodate only small amounts of polyamines, with the basic alumina having the lowest loading. This also indicates that besides silica supports, polyamines can be grown on other oxides such as alumina. In general, the polymerization of these cyclic amines by vapor-phase transport appears applicable to any support containing acidic hydroxyl groups on their surface that can facilitate the ring-opening reaction.

Figure 5 shows nitrogen adsorption–desorption isotherms and the corresponding NL-DFT pore size distributions of the

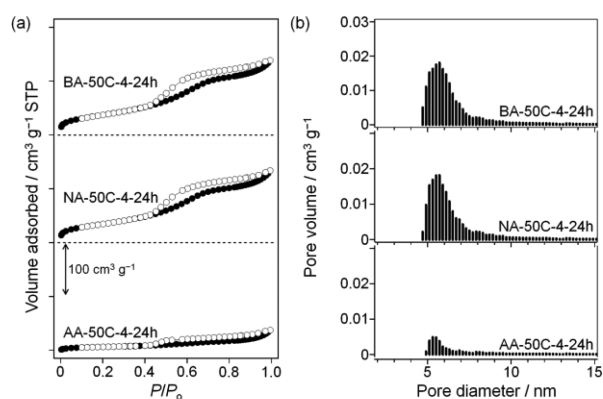


**Figure 5.** (a) Nitrogen adsorption–desorption isotherms (filled and empty symbols representing adsorption and desorption branches, respectively) and (b) the corresponding histograms of NL-DFT pore size distribution of the resulting hybrids prepared on alumina supports. The isotherms of NA-50C-4-24h and BA-50C-4-24h were offset by 200 and 400 cm<sup>3</sup> g<sup>-1</sup> STP, respectively.

resulting hybrid materials. The isotherms and pore size distributions of the hybrid materials prepared on the neutral and basic alumina supports were almost identical to those of the bare supports (see Supporting Information, Figure S6). In contrast, nitrogen adsorption drastically decreased for the hybrid prepared on the acidic alumina support, with the NL-DFT pore diameter being smaller than that of the parent support. These results additionally support the notion that support acidity strongly influences the formation of supported polyamines via ring-opening polymerization. It should be noted that the coexistence of Lewis acid sites in the Al-grafted SBA-15 and alumina supports may also affect the ring-opening

polymerization of aziridines, as Lewis acids are known to catalyze nucleophilic addition reactions, especially for substituted aziridines.<sup>9</sup> For unsubstituted aziridine used here, however, the initiation reaction for the ring-opening polymerization is likely the formation of the cationic aziridinium intermediates that are more easily formed with Brønsted acids. At this stage, it remains unclear how supported Lewis acid sites affect the ring-opening polymerization of aziridines under the vapor-phase conditions investigated here.

#### Characteristics of the Supported Poly(ethylenimine).

The degree of polymerization and branching of the supported polyamines were evaluated. The supported polyamines were cleaved from their supports by dissolution of the silica framework in concentrated alkali solution. The molecular weights of the cleaved polyamines were determined by aqueous gel permeation chromatography (size exclusion chromatography) using commercial poly(ethylenimine)s as standards. As reported in Table 3, the obtained polyamines possessed low

**Table 3. Molecular Weights and Degrees of Branching of the Cleaved Poly(ethylenimine)s**

sample	$N_{\text{TGA}}$ (mmol g <sup>-1</sup> )	molecular weight (Da)	amine ratio <sup>b</sup> 1°:2°:3°
S-23C-4-24h	3.66	(100) <sup>a</sup>	31:42:27
S-50C-4-24h	7.38	530	31:40:29
S-60C-4-24h	8.15	620	32:39:29
S-70C-4-24h	9.66	950	32:39:29
S-80C-4-24h	9.83	1060	32:39:29
AS-70C-4-24h	10.12	1960	30:43:27

<sup>a</sup>This calculated value was much lower than those for the standard polymers and should be considered only in a qualitative manner. Also, this value seems to be lower than the detection limit in our chromatography instrument. <sup>b</sup>Represented as a percentage ratio of primary: secondary: tertiary amines.

molecular weights, up to 1960 Da. These values are in sharp contrast to the hyperbranched polyamines polymerized via the standard liquid-phase reaction, which were previously reported to have the molecular weights of 4500–6500 Da.<sup>8b,c</sup> Although the molecular level details remain unclear, the polymerization and termination rates of poly(ethylenimine)s grown via the vapor-phase transport method are likely different from those that occur in the liquid-phase polymerization. One possible explanation is that the swelling of polymer may strongly affect the growth of polymer, as the swelling would enhance the exposure of polymer ends to attack the heterocyclic monomers, thereby resulting in the elongation of the polymer chains. The swelling may be suppressed under the vapor-phase conditions, giving the lower molecular weight polyamines.

Figure 6 shows the molecular weights of the cleaved polyamines as a function of the amine content of the hybrid materials. This set of hybrid materials was synthesized at the same aziridine/support ratio and synthesis time. As discussed above, hybrid materials with higher polyamine loadings were obtained from experiments at higher synthesis temperatures. Therefore, the observed parabolic increase in molecular weights as the amine content and synthesis temperature increased suggests that the higher synthesis temperature enhanced the degree of polymerization. Moreover, the material prepared on the Al-grafted SBA-15 support (i.e., AS-70C-4-24h) had a much higher molecular weight than those prepared on the SBA-15 support, again indicating that the acidity of support promotes

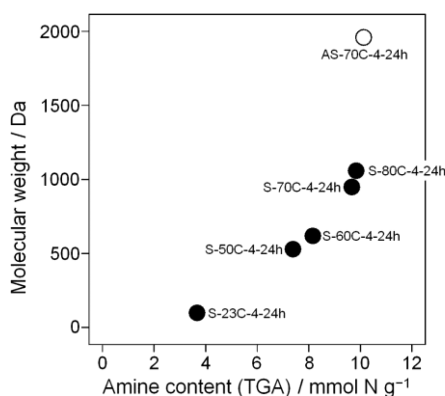


**Figure 6.** Relation between molecular weights of the cleaved poly(ethylenimine)s and amine contents of the corresponding hybrid materials prepared on the SBA-15 (filled symbols) and the Al-grafted SBA-15 (empty symbols) supports.

the polymerization and subsequently leads to a higher degree of polymerization.

Solution-state  $^{13}\text{C}$  NMR with inversely gated decoupling was employed to quantify the degree of polymer branching. As illustrated in Figure 7a, there are eight different carbon atom

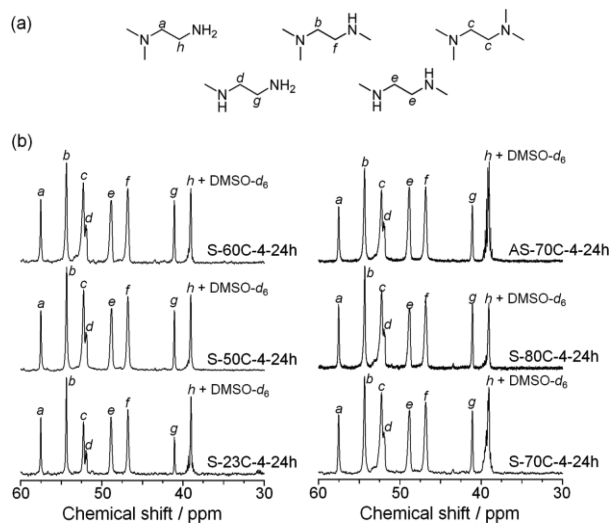


**Figure 7.** (a) Eight different environments of carbon atoms in poly(ethylenimine). (b) Inversely gated solution-state  $^{13}\text{C}$  NMR spectra of the cleaved poly(ethylenimine)s from various hybrid materials.

environments in the poly(ethylenimine). Figure 7b shows the inversely gated  $^{13}\text{C}$  NMR spectra of the cleaved polyamines. Note that  $\text{Cr}(\text{acac})_3$  in  $\text{DMSO}-d_6$  was added to the sample solution as a paramagnetic relaxation agent to attain high resolution spectra, as it aids relaxation by shortening the carbon  $T_1$  decay times and minimizes interference from residual silica or base after the polymer cleavage from the support. Unfortunately, the signal of the  $\text{DMSO}-d_6$  NMR solvent somewhat overlaps with the signal from the carbon at the h position. To determine the amine ratio, the peak area of the h-carbon was assumed to be equal to that of the a-carbon, because both carbons are present in the same fragment of the polyamine and their peak areas should then be identical.<sup>23a</sup> The molar ratios of primary, secondary, and tertiary amines of the cleaved polyamines were quantitatively analyzed from the NMR

peak areas and are summarized in Table 3. The results are slightly altered from the average ratio of  $1^\circ:2^\circ:3^\circ = 28:46:26$  for the supported polyamines prepared by the liquid-phase methods reported previously,<sup>8b</sup> with the hybrid materials prepared here having slightly higher and lower fractions of primary and secondary amines, respectively. The ratios persist across various samples, indicating that the degree of polyamine branching was not significantly impacted by the synthesis conditions and supports.

**CO<sub>2</sub> Adsorption.** CO<sub>2</sub> adsorption measurement using the resulting hyperbranched poly(ethylenimine)-oxide hybrids was performed under dry conditions using a simulated flue gas (10% CO<sub>2</sub> balanced with helium) to evaluate their performance in comparison with similar materials prepared in liquid media reported previously. The pseudoequilibrium CO<sub>2</sub> adsorption capacities and amine efficiencies, defined as the number of moles of CO<sub>2</sub> captured per mole of active amines, of the resulting materials are summarized in Table 4. It is noteworthy

**Table 4.** CO<sub>2</sub> Adsorption Capacities under Dry Conditions Using Simulated Flue Gas (10% CO<sub>2</sub>)

sample	$N_{\text{TGA}}$ (mmol g <sup>-1</sup> )	capacity (mmol CO <sub>2</sub> g <sup>-1</sup> )	amine efficiency (mol CO <sub>2</sub> per mol N)
S-70C-1-24h	6.19	0.69	0.11
S-23C-4-168h	6.33	0.73	0.12
S-70C-2-24h	7.23	0.93	0.13
AS-50C-4-24h	7.52	0.70	0.09
S-70C-4-24h	9.66	0.43	0.04
<i>Hyperbranched Poly(ethylenimine)-SBA-15 Hybrid Prepared by the Standard Liquid-Phase Method<sup>8</sup></i>			
liquid-HAS	5.44	0.58	0.11
<i>Poly(ethylenimine)-Impregnated SBA-15</i>			
PEI/SBA-15 <sup>5g</sup>	7.40	0.65	0.09

that under dry conditions only primary and secondary amines are expected to react with CO<sub>2</sub> to produce carbamates through the formation of zwitterionic intermediates.<sup>5</sup> In this mechanism, an additional free base is required per mole of CO<sub>2</sub> captured for deprotonating the zwitterions to form the carbamates. As a result, the theoretical maximum amine efficiency for poly(ethylenimine)-based materials under dry conditions is varied from 0.35 to 0.5, depending on the amount of tertiary amines.<sup>5,8,12</sup> At low amine loadings, the CO<sub>2</sub> adsorption capacities and amine efficiencies of the resulting hybrids increased as the amine content increased. At the higher amine loadings in which some pore spaces were blocked or closed (vide supra), however, the capacities and amine efficiencies were lowered. This is likely because the CO<sub>2</sub> molecules cannot easily diffuse to access all the amines in the interior of these materials because of the presence of polyamines grown near/in the pore mouths and the steric hindrances caused by the previously formed (cross-linking) carbamates.<sup>5</sup> As can be seen, the poly(ethylenimine)-oxide hybrid materials prepared here are as efficient in CO<sub>2</sub> adsorption as the related materials prepared by the standard liquid-phase method, as well as materials made by physically impregnating SBA-15 with poly(ethylenimine), suggesting that the vapor-phase method is an effective way to produce CO<sub>2</sub>-adsorbing polyamines. It should be noted that the CO<sub>2</sub> adsorption performance of this class of materials can be substantially improved under wet conditions, as reported previously.<sup>5a,8</sup>

### Hyperbranched Poly(propylenimine)-Oxide Hybrid.

Polyamines with different lengths of methylene spacers between the amine groups may affect the material stability and performance in some applications such as catalysis and CO<sub>2</sub> capture.<sup>2f</sup> A SBA-15-supported poly(propylenimine) material was also prepared via the vapor-phase transport using azetidine monomer (see Scheme 1) with an azetidine/SBA-15 mass ratio of 4 at 80 °C for 24 h. The polyamine loading was calculated from the TGA weight loss to be about 15 wt %. The powder XRD pattern of the resulting material (see Supporting Information, Figure S7a) indicates that the 2D hexagonal mesostructure of the material was maintained, as in the case of materials made with aziridine. The DTG curve depicted in the Supporting Information, Figure S7b, shows a peak at 245 °C, which is 25 °C higher than the peaks seen in the supported poly(ethylenimine) materials, suggesting the supported poly(propylenimine) is thermally more stable than its poly(ethylenimine) counterparts. Nitrogen adsorption–desorption isotherms and the corresponding NL-DFT pore size distribution are shown in the Supporting Information, Figures S7c and S7d, respectively. The BET surface area and total pore volume were calculated to be 334 m<sup>2</sup> g<sup>-1</sup> and 0.68 cm<sup>3</sup> g<sup>-1</sup>, respectively. The resulting poly(propylenimine) hybrid material had lower organic loading than the poly(ethylenimine) material prepared under the same conditions, most likely because azetidine has a lower vapor pressure (i.e., higher boiling point) and less ring strain than aziridine.<sup>9</sup> The loading of the poly(propylenimine) may be improved by preparing materials at harsher conditions. Optimization of synthesis conditions to attain higher poly(propylenimine) loadings merits investigation in future work.

### CONCLUSIONS

Preparation of supported hyperbranched polyamine-oxide hybrid materials via vapor-phase transport was demonstrated for the first time. In contrast to the conventional liquid-phase method reported previously,<sup>7,8,10</sup> in which the supports are dispersed in an organic solvent (typically toluene) containing the cyclic monomers, in the vapor-phase method, the liquid monomers and the solid supports are placed separately in an enclosed environment. The cyclic amine monomers were then transported onto the support surface in the vapor-phase by heating the vessel containing the monomer and support. Ring-opening polymerization then occurs on the support surface, resulting in polyamines covalently tethered to the supports. The data shown here suggest that this method can be carried out over a wide range of preparation conditions, with different oxide supports, and with different cyclic amine monomers. Compared to related materials reported thus far, a hybrid material with the highest poly(ethylenimine) loading was achieved by the vapor-phase method. Interestingly, the resulting supported poly(ethylenimine)s possessed lower molecular weights than the previously reported materials prepared by the liquid-phase method. The acidity of supports clearly promoted the polymerization, with more acidic supports resulting in the hybrid materials with higher polyamine loadings and degrees of polymerization. This vapor-phase method is anticipated to effectively introduce covalently bound polyamines onto structured contactors such as tubular membranes and monoliths, thereby facilitating possible use in large scale applications in a scalable manner.

### ASSOCIATED CONTENT

#### Supporting Information

Experimental setup, detailed characterizations of the SBA-15, Al-grafted SBA-15, and alumina supports, FE-SEM images and differential TGA curves of the hybrids, and XRD pattern, differential TGA curve, N<sub>2</sub> sorption isotherms and NL-DFT pore size distribution of the hyperbranched poly(propylenimine)-oxide hybrid material. This material is available free of charge via the Internet at <http://pubs.acs.org>.

### AUTHOR INFORMATION

#### Corresponding Author

\*E-mail: [cjones@chbe.gatech.edu](mailto:cjones@chbe.gatech.edu).

#### Present Address

<sup>†</sup>World Premier International (WPI) Research Center for Materials Nanoarchitectonics (MANA), National Institute for Materials Science, 1-1 Namiki, Tsukuba, Ibaraki, 305-0044 Japan.

#### Notes

The authors declare the following competing financial interest(s): C.W.J. has a financial interest in Global Thermostat, LLC.

### ACKNOWLEDGMENTS

We thank Global Thermostat, LLC and School of Chemical & Biomolecular Engineering at Georgia Tech (through the New-Vision Professorship awarded to C.W.J.) for financial support.

### REFERENCES

- (1) (a) Hoffmann, F.; Cornelius, M.; Morell, J.; Fröba, M. *Angew. Chem., Int. Ed.* **2006**, *45*, 3216–3251. (b) Soler-Illia, G. J. A. A.; Innocenzi, P. *Chem.—Eur. J.* **2006**, *12*, 4478–4494. (c) Fujita, S.; Inagaki, S. *Chem. Mater.* **2008**, *20*, 891–908. (d) Yamamoto, K.; Tatsumi, T. *Chem. Mater.* **2008**, *20*, 972–980. (e) Hu, L.-C.; Shea, K. J. *Chem. Soc. Rev.* **2011**, *40*, 688–695. (f) Linares, N.; Serrano, E.; Rico, M.; Balu, A. M.; Losada, E.; Luque, R.; García-Martínez, J. *Chem. Commun.* **2011**, *47*, 9024–9035.
- (2) (a) Margelefsky, E. L.; Zeidan, R. K.; Davis, M. E. *Chem. Soc. Rev.* **2008**, *37*, 1118–1126. (b) Wang, Q.; Guerrero, V. V.; Ghosh, A.; Yeu, S.; Lunn, J. D.; Shantz, D. F. *J. Catal.* **2010**, *269*, 15–25. (c) Kubota, Y.; Yamaguchi, H.; Yamada, T.; Inagaki, S.; Sugi, Y.; Tatsumi, T. *Top. Catal.* **2010**, *53*, 492–499. (d) Das, S.; Asefa, T. *ACS Catal.* **2011**, *1*, 502–510. (e) Fihri, A.; Bouhrara, M.; Patil, U.; Cha, D.; Saih, Y.; Polshettiwar, V. *ACS Catal.* **2012**, *2*, 1425–1431. (f) Brunelli, N. A.; Didas, S. A.; Venkatasubbaiah, K.; Jones, C. W. *J. Am. Chem. Soc.* **2012**, *134*, 13950–13953.
- (3) (a) Yoshitake, H.; Yokoi, T.; Tatsumi, T. *Chem. Mater.* **2003**, *15*, 1713–1721. (b) Yoo, S.; Lunn, J. D.; Gonzalez, S.; Ristich, J. A.; Simanek, E. E.; Shantz, D. F. *Chem. Mater.* **2006**, *18*, 2935–2942. (c) Walcarius, A.; Mercier, L. *J. Mater. Chem.* **2010**, *20*, 4478–4511. (d) Yoshitake, H. *J. Mater. Chem.* **2010**, *20*, 4537–4550.
- (4) (a) Gu, J.; Fan, W.; Shimojima, A.; Okubo, T. *Small* **2007**, *3*, 1740–1744. (b) Budi Hartono, S.; Qiao, S. Z.; Jack, K.; Ladewig, B. P.; Hao, Z.; Lu, G. Q. *Langmuir* **2009**, *25*, 6413–6424. (c) Tran, D. N.; Balkus, K. J., Jr. *ACS Catal.* **2011**, *1*, 956–968. (d) Suteewong, T.; Sai, H.; Cohen, R.; Wang, S.; Bradbury, M.; Baird, B.; Gruner, S. M.; Wiesner, U. *J. Am. Chem. Soc.* **2011**, *133*, 172–175.
- (5) (a) Bollini, P.; Didas, S. A.; Jones, C. W. *J. Mater. Chem.* **2011**, *21*, 15100–15120. (b) Chaikittisilp, W.; Lunn, J. D.; Shantz, D. F.; Jones, C. W. *Chem.—Eur. J.* **2011**, *17*, 10556–10561. (c) Chaikittisilp, W.; Kim, H.-J.; Jones, C. W. *Energy Fuels* **2011**, *25*, 5528–5537. (d) Wang, L.; Yang, R. T. *J. Phys. Chem. C* **2011**, *115*, 21264–21272. (e) Didas, S. A.; Kulkarni, A. R.; Sholl, D. S.; Jones, C. W. *ChemSusChem* **2012**, *5*, 2058–2064. (f) Sayari, A.; Heydari-Gorji, A.; Yang, Y. *J. Am. Chem. Soc.* **2012**, *134*, 13834–13842. (g) Kuwahara, Y.; Kang, D.-Y.;

Copeland, J. R.; Brunelli, N. A.; Didas, S. A.; Bollini, P.; Sievers, C.; Kamegawa, T.; Yamashita, H.; Jones, C. W. *J. Am. Chem. Soc.* **2012**, *134*, 10757–10760.

(6) (a) Lunn, J. D.; Shantz, D. F. *Chem. Mater.* **2009**, *21*, 3638–3648. (b) Subra, G.; Mehdi, A.; Enjalbal, C.; Amblard, M.; Brunel, L.; Corriu, R.; Martinez, J. J. *Mater. Chem.* **2011**, *21*, 6321–6326.

(7) (a) Rosenholm, J. M.; Penninkangas, A.; Lindén, M. *Chem. Commun.* **2006**, 3909–3911. (b) Rosenholm, J. M.; Lindén, M. *Chem. Mater.* **2007**, *19*, 5023–5034. (c) Rosenholm, J. M.; Duchanoy, A.; Lindén, M. *Chem. Mater.* **2008**, *20*, 1126–1133.

(8) (a) Hicks, J. C.; Drese, J. H.; Fauth, D. J.; Gray, M. L.; Qi, G.; Jones, C. W. *J. Am. Chem. Soc.* **2008**, *130*, 2902–2903. (b) Drese, J. H.; Choi, S.; Lively, R. P.; Koros, W. J.; Fauth, D. J.; Gray, M. L.; Jones, C. W. *Adv. Funct. Mater.* **2009**, *19*, 3821–3832. (c) Drese, J. H.; Choi, S.; Didas, S. A.; Bollini, P.; Gray, M. L.; Jones, C. W. *Microporous Mesoporous Mater.* **2012**, *151*, 231–240.

(9) (a) Padwa, A. In *Comprehensive Heterocyclic Chemistry III*; Katritzky, A. R., Ramsden, C. A., Scriven, E. F. V., Taylor, R. J. K., Eds.; Elsevier: Amsterdam, The Netherlands, 2008; Vol. 1, pp 1–105. (b) Dermer, O. C.; Ham, G. E. *Ethylenimine and Other Aziridines*; Academic Press: New York, 1969. (c) Goethals, E. J.; Schacht, E. H.; Bogaert, Y. E.; Ali, S. I.; Tezuka, Y. *Polym. J.* **1980**, *12*, 571–581. (d) Hu, X. E. *Tetrahedron* **2004**, *60*, 2701–2743.

(10) (a) Kim, H. J.; Moon, J. H.; Park, J. W. *J. Colloid Interface Sci.* **2000**, *227*, 247–249. (b) Kim, C. O.; Cho, S. J.; Park, J. W. *J. Colloid Interface Sci.* **2003**, *260*, 374–378.

(11) Drese, J. H.; Talley, A. D.; Jones, C. W. *ChemSusChem* **2011**, *4*, 379–385.

(12) Choi, S.; Drese, J. H.; Eisenberger, P. M.; Jones, C. W. *Environ. Sci. Technol.* **2011**, *45*, 2420–2427.

(13) (a) Kulkarni, A. R.; Sholl, D. S. *Ind. Eng. Chem. Res.* **2012**, *51*, 8631–8645. (b) Bollini, P.; Brunelli, N. A.; Didas, S. A.; Jones, C. W. *Ind. Eng. Chem. Res.* **2012**, *51*, 15145–15152.

(14) (a) Lively, R. P.; Chance, R. R.; Kelley, B. T.; Deckman, H. W.; Drese, J. H.; Jones, C. W.; Koros, W. J. *Ind. Eng. Chem. Res.* **2009**, *48*, 7314–7324. (b) Gebald, C.; Wurzbacher, J. A.; Tingaut, P.; Zimmermann, T.; Steinfeld, A. *Environ. Sci. Technol.* **2011**, *45*, 9101–9108.

(15) (a) Winther-Jensen, B.; West, K. *Macromolecules* **2004**, *37*, 4538–4543. (b) O'Connell, C. D.; Higgins, M. J.; Nakashima, H.; Moulton, S. E.; Wallace, G. G. *Langmuir* **2012**, *28*, 9953–9960.

(16) (a) Nishiyama, N.; Tanaka, S.; Egashira, Y.; Oku, Y.; Ueyama, K. *Chem. Mater.* **2003**, *15*, 1006–1011. (b) Tanaka, S.; Nishiyama, N.; Oku, Y.; Egashira, Y.; Ueyama, K. *J. Am. Chem. Soc.* **2004**, *126*, 4854–4858.

(17) Yamauchi, Y.; Takai, A.; Komatsu, M.; Sawada, M.; Ohsuna, T.; Kuroda, K. *Chem. Mater.* **2008**, *20*, 1004–1011.

(18) Causey, D. H.; Mays, R. P.; Shamblee, D. A.; Lo, Y. S. *Synth. Commun.* **1988**, *18*, 205–211.

(19) Zhao, D.; Huo, Q.; Feng, J.; Chmelka, B. F.; Stucky, G. D. *J. Am. Chem. Soc.* **1998**, *120*, 6024–6036.

(20) Li, Q.; Wu, Z.; Tu, B.; Park, S. S.; Ha, C.-S.; Zhao, D. *Microporous Mesoporous Mater.* **2010**, *135*, 95–104.

(21) Ravikovitch, P. I.; Neimark, A. V. *J. Phys. Chem. B* **2001**, *105*, 6817–6823.

(22) Brunelli, N. A.; Venkatasubbiah, K.; Jones, C. W. *Chem. Mater.* **2012**, *24*, 2433–2442.

(23) (a) St Pierre, T.; Geckle, M. J. *Macromol. Sci., Chem.* **1985**, *22*, 877–887. (b) von Harpe, A.; Petersen, H.; Li, Y.; Kissel, T. J. *Controlled Release* **2000**, *69*, 309–322.

(24) The bare SBA-15 support used entirely in the present study has a BET surface area of 920 m<sup>2</sup> g<sup>-1</sup>, total pore volume (at  $P/P_0 = 0.99$ ) of 1.07 cm<sup>3</sup> g<sup>-1</sup>, and micropore volume (determined by the  $t$ -plot method) of 0.11 cm<sup>3</sup> g<sup>-1</sup>.

(25) Brinker, C. J.; Scherer, G. W. *Sol–Gel Science: The Physics and Chemistry of Sol–Gel Processing*; Academic Press: San Diego, CA, 1990.

(26) The Al-grafted SBA-15 support used in the present study possessed a BET specific surface area of 715 m<sup>2</sup> g<sup>-1</sup>, total pore volume

(at  $P/P_0 = 0.99$ ) of 0.89 cm<sup>3</sup> g<sup>-1</sup>, and micropore volume (determined by the  $t$ -plot method) of 0.07 cm<sup>3</sup> g<sup>-1</sup>.

(27) Acidic, neutral, and basic activated aluminas were obtained from a commercial source. These materials have almost identical textural properties with BET specific surface areas of 143, 154, and 164 m<sup>2</sup> g<sup>-1</sup> (the values in catalog are all 150 m<sup>2</sup> g<sup>-1</sup>) and total pore volumes (at  $P/P_0 = 0.99$ ) of 0.23, 0.24, and 0.25 cm<sup>3</sup> g<sup>-1</sup>, respectively.